

Adhesive Tack in Bonding and Debonding



MIZUMACHI Hiroshi
Professor Emeritus
The University of Tokyo

1964
 Completed Master's Degree
 in Applied Chemistry,
 Graduate School of
 Engineering, Kyushu
 University

1969
 Associate Professor,
 Department of Agriculture,
 Shizuoka University

1978
 Associate Professor,
 Department of Agriculture,
 The University of Tokyo

1985
 Professor, The University of
 Tokyo

1998
 Professor Emeritus, The
 University of Tokyo

1999
 Project Coordinator,
 Fukuoka Industry, Science
 and Technology Foundation

1992-1994
 President, The Adhesion
 Society of Japan

1996-1998
 President, The Society of
 Packaging Science and
 Technology, Japan

Research field: adhesion science

1. Introduction

Tack, which denotes the ability of adhesive agents to form bonds instantaneously, is one of their most important practical characteristics. While various empirical rules¹⁾ have been expounded regarding the phenomenon of tack, its precise mechanism is still not satisfactorily understood. The elementary processes of the tack phenomenon are the bonding and debonding processes between the adhesive and the substrate. The contribution of each of these is believed to vary according to measurement method and ambient conditions, which makes it very complex and difficult to quantify on a scientific basis.

The authors have researched a method of measuring adhesive tack and developed a related rheological theory. The present paper gives a brief summary of the features of tack followed by a discussion of the contribution of the bonding and debonding processes from a simplified theoretical standpoint.

2. Adhesive Tack

2.1 Ball Tack

(a) Ball tack and rolling friction coefficient

Adhesive tack is often measured using the rolling ball method of which the J. Dow version and the PSTC-6 version are the most common. The authors²⁾⁻⁴⁾ analyzed dynamically the motion of a rigid ball and, using a combination of fundamental equation (1) below and equation (2), which expresses the velocity dependence of the rolling friction coefficient f , found that the equations resulting from their combination reproduced with a very high degree of accuracy experimentally measured data on velocity, distance traveled, and rollout distance.

$$d^2x/dt^2 = - 5gf/7R \tag{1}$$

$$f = f_0 + f_1v \tag{2}$$

where x is distance traveled by ball, g is acceleration of gravity, f is rolling friction coefficient, R is radius of ball, f_0, f_1 are constants, and v is dx/dt .

Figure 1 provides an example. The figure shows the analytical results from an experiment in

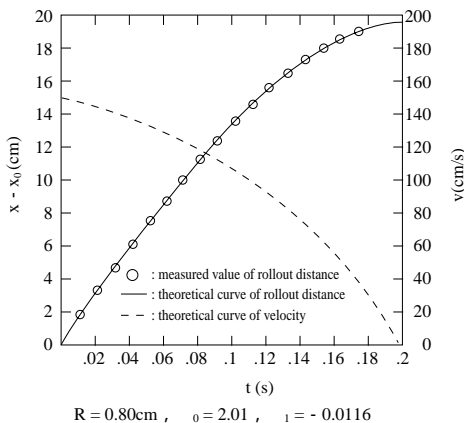


Fig. 1 Rigid ball rolling on cloth packaging tape surface

which a steel ball was allowed to roll on the surface of commercially available cloth packaging tape and its position registered every 0.1 seconds by a stroboscopic photography. If one assumes that the rolling friction coefficient f of this tape is $f=0.8-0.016v$, a theoretical curve can be drawn connecting all measured values. Another distinctive feature is that all measured values fall within the range $v = 10\sim 10^2$ cm/sec and that values for rollout distance, as calculated using parameters ($\mu_0=0.8, \mu_1=-0.016$) evaluated from data within this range, accurately match the actual measured values.

After conducting analysis of this kind on many different commercial adhesive tapes, it was possible to determine their rolling friction coefficient f , or the parameters μ_0 and μ_1 .

This fact indicates that the regular rolling ball method of allowing a rigid ball to roll on an adhesive surface and seeing how far it rolls before coming to rest corresponds to measuring rolling friction coefficient of adhesive agents within a relatively narrow range of velocities. In other words, the practical properties expressed as ball tack show performance within the velocities range $10\sim 10^2$ cm/sec (in order to expand the velocity range by one digit it would be necessary to increase ball drop height 100-fold).

In many packaging tapes, masking tapes, cellophane tapes and other tapes, rolling friction coefficient tends to drop as velocity increases ($\mu_1 < 0$), but in some packaging and medical tapes, the opposite tendency is seen ($\mu_1 > 0$).

(b) Measurement of rolling friction coefficient using pulling cylinder method

We have seen that the rolling ball method for evaluating adhesive tack is actually a method for measuring the rolling friction coefficient of the adhesive, but as rolling friction coefficient depends on velocity, in order to analyze the data, it is necessary to establish an assumption such as that represented by equation (2). However, by pulling a ball or cylinder of radius R and mass M at a fixed velocity over the adhesive surface and measuring the resistance P , it is simple to calculate the rolling friction coefficient corresponding to that velocity, as in equation (3) below:

$$f = PR/Mg \tag{3}$$

In this case there is no need to make any assumption regarding velocity dependency of rolling friction coefficient.

Using the pulling cylinder method, the authors^{5), 6)} measured the temperature and velocity dependency of rolling friction coefficient. The rolling friction coefficient of adhesive at a constant temperature, like other adhesive properties, describes a curve with a maximum value at a certain velocity; if the measuring temperature rises, the curve shifts to the high-velocity side. Also, if the thickness of the adhesive layer is increased, the maximum value shifts to the high-velocity side and at the same time absolute value increases slightly. These features are illustrated in Fig. 2.

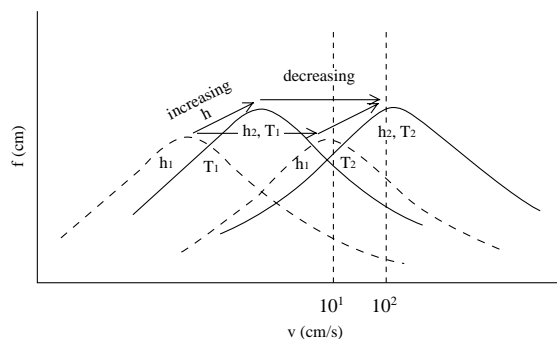


Fig. 2 Velocity dependence of rolling friction coefficient f of adhesive (schematic representation)

On the low-velocity side of the peak, cohesive failure of the adhesive is mainly seen, while on the high-velocity side interfacial failure is observed.

The assumption $f = f_0 + f_1 v$ established when analyzing the data from the rolling ball method was equivalent to superimposing a straight line on the $v = 10 \sim 10^2$ cm/sec section of this curve.

For adhesives in the case of which the rolling friction coefficient obtained using the pulling cylinder method in this velocity range describes a rising curve (i.e. $df/dv > 0$), it has been demonstrated that the rolling ball method also produces $f_1 > 0$, while for those with a falling curve it produces $f_1 < 0$.

When rolling friction coefficient defined in dynamic terms is measured for adhesive agents, the curve in Fig. 2 is obtained, but when the regular rolling ball methods such as the J. Dow method and the PSTC-6 method are used, the behavior seen represents only a very narrow velocity range ($v = 10 \sim 10^2$ cm/sec). To put it another way, the practical properties called tack coincide with this rolling friction coefficient at this velocity range; the further velocity falls below the threshold of this velocity range, the closer rolling friction coefficient should tend toward peeling.

(c) Dependence of rolling friction coefficient and peeling force on critical surface tension (γ_c) of adherend

If rolling friction coefficient is measured over a wide range of velocity, it becomes clear that a marked dependence on the critical surface tension (γ_c) of the adherend (i.e. the cylinder) appears, especially in the high-velocity range where interfacial failure occurs. A typical example of this is shown in Fig. 3, which describes the rolling friction coefficient of a 90/10 copolymer of butyl acrylate and acrylic acid. The distinctive features of this figure are that a peak appears in the range where cohesive failure occurs, followed by a second peak in the range where interfacial failure occurs, and the higher critical surface tension of the cylinder becomes, the higher the latter peak becomes⁷⁾. These features can be explained qualitatively using a simplified rheological theory^{8), 9)}.

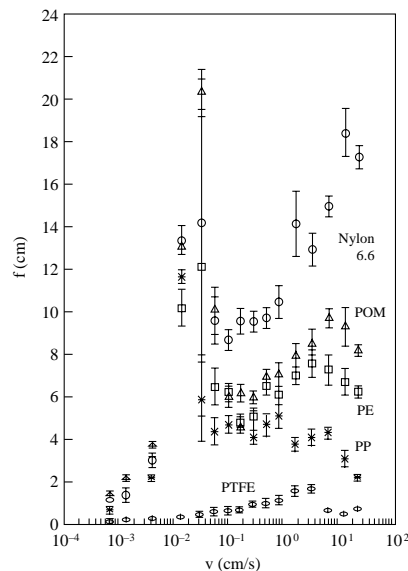


Fig. 3 Velocity dependence of rolling friction coefficient f of acrylic adhesive (butyl acrylate 90/acrylic acid 10)

2.2 Probe Tack

The probe tack of adhesive can be evaluated by bringing the smooth end of a cylindrical probe into contact with the adhesive and then plotting the curve of stress/strain produced when it is pulled away. The degree of tack is often expressed as the maximum stress value (σ_{max}), but Zosel¹⁰⁾ claims that adhesive energy (W_{adh}) should be calculated as the area under the stress/distortion curve and that this represents a clearer index of tack in terms of physical science.

Kim¹¹⁾ measured the probe tack of many blends of acrylic copolymer with tackifier and discovered that these two parameters had slightly differing features. Regarding maximum stress, the superposition of temperature over velocity was very good, delivering the master curve shown in

Fig. 4; the higher the T_g of the adhesive, the more the peak shifted to the low-velocity side. Regarding adhesive energy, the tendency was basically the same, but the superposition of temperature over velocity was unsatisfactory in some cases.

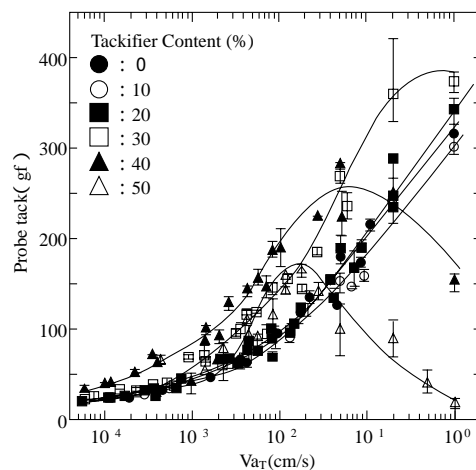


Fig. 4 Dependence on pulling-away velocity of σ_{max} in probe tack of acrylic adhesive (blend of acrylic copolymer and rosin tackifier)

Creton *et al*¹²⁾ observed the same tendency and interpreted it as follows: when the cylinder is pulled away, at first a uniform deformation arises, but then cavities develop at the adhesive surface and begin to expand. Since maximum stress appears during this initial stage while strain is still low, it displays a tendency similar to linear visco-elasticity. However, towards the end of the pulling away process, fibril structures develop. The energy which is dissipated with the growth of the fibril structures contributes greatly to adhesive energy (accounting for 70~90% thereof depending on the velocity range of measurement). Because this corresponds to the great deformation arising from nonlinear visco-elasticity, it is difficult to predict all of these properties directly from elastic modulus alone.

The stress/strain curve can be obtained by the probe tack test and information about the mechanism of adhesive failure and changes therein can be obtained from the curve.

Zosel¹³⁾ demonstrated that uniform deformation produces a very sharp peak while fibrillation produces a sharp peak followed by a curve with a flattened section; and that if, under constant temperature, pulling away is performed at various velocities, as shown in Fig. 5, at a certain velocity, a clear transition from uniform deformation to fibrillation is observed. Ga in this figure corresponds to W_{adh} . Creton *et al.*¹²⁾ classified the patterns of the stress/strain curve more finely (Fig. 6), and reported that the various curves appeared in the so-called “viscoelastic window” (a

certain temperature-velocity range) of the adhesive agent (Fig. 7). Creton *et al.* also demonstrated that the shape of the stress/strain curve in the probe tack test changes considerably at low temperature, and concluded that these temperature ranges provoked behaviors dependent on the contact process. At this stage, time comes into play as a new factor, so that the velocity/temperature superposition no longer holds for probe tack.

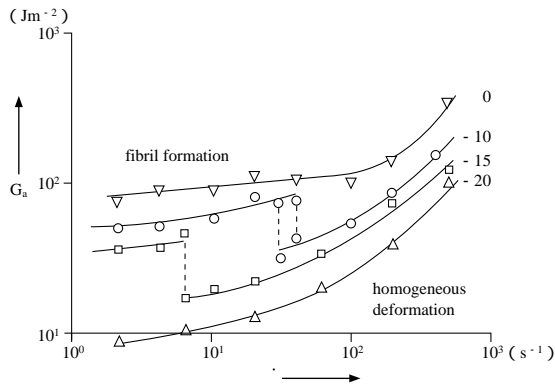


Fig. 5 Dependence on pulling away velocity of adhesive energy G_a (corresponding to W_{adh})
Transition from uniform deformation to fibril formation found to occur at certain velocity (Zosel)

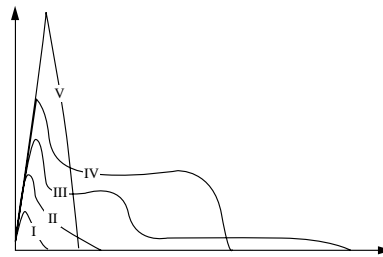


Fig. 6 Typical stress/strain curve in probe tack test (Creton *et al.*)

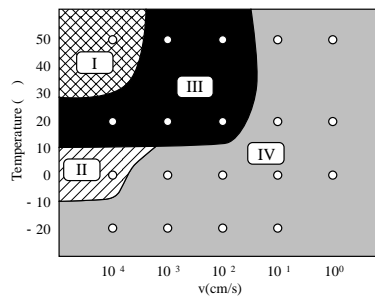


Fig. 7 Region of temperature/velocity flattening in which typical stress/strain curve occurs (Creton *et al.*) Adhesive: poly 2-ethyl hexyl acrylate

3. Tack in Bonding and Debonding

It is known that bonding and debonding contribute simultaneously to adhesive tack. Since both processes are velocity-dependent, for both probe tack and rolling friction coefficient, the relative contribution of the two will naturally differ depending on the time scale of measurement. This is proved in the following¹⁴).

Figures 8 and 9 show the master curves of rolling friction coefficient for acrylic adhesive (90/10 copolymer of butyl acrylate and acrylic acid). The two adhesive samples were in the form of double-sided adhesive tape covered on either side with release liner. The copolymer composition, molecular weight, and molecular weight distribution of the adhesives were confirmed equal, but a different release liner was used on the two samples and precise data on this factor is not available. The adhesive was applied to a glass plate and the velocity dependence of rolling friction coefficient measured at various temperatures using the pulling cylinder method, and a master curve was plotted by shifting the curves so that they became superposed at the low-velocity side (the side where cohesive failure occurs). The adhesive in Fig. 8 (PSA-N) produced a relatively neat curve at all velocity ranges, but with the adhesive of Fig. 9 (PSA-T), the superposition at the high-velocity side (where interfacial failure occurs) is not satisfactory.

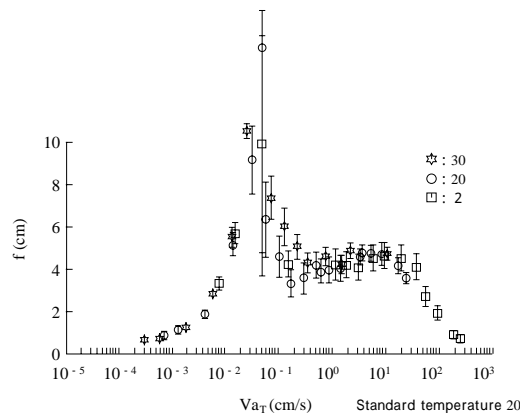


Fig. 8 Master curve of rolling friction coefficient of acrylic adhesive PSA-N (90/10 copolymer of butyl acrylate and acrylic acid)

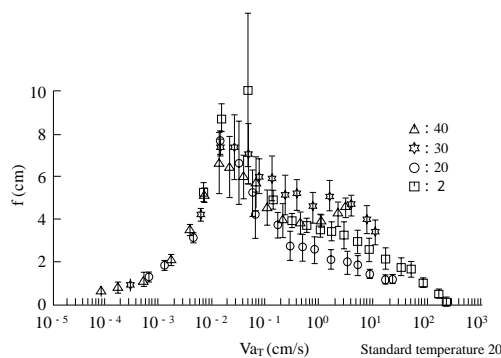


Fig. 9 Master curve of rolling friction coefficient of acrylic adhesive PSA-T (copolymer composition as in Fig. 8)

As shown in Fig. 10, the shift factor a_T necessary to superpose the low-velocity section of the curves is the same for the two adhesives, and activating energy is calculated to be around 20 kcal/mole. This is thought to correspond to the activation energy of the debonding process, $\Delta H^*_{\text{debond}}$.

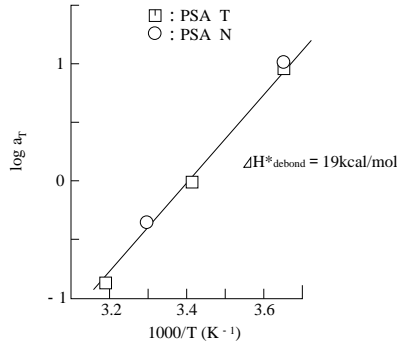


Fig. 10 Arrhenius plot of shift factor a_T in superposing of low-velocity sections of rolling friction coefficients of PSA-N and PSA-T

In the low-velocity range, when the bonding process is sufficiently advanced, the debonding process begins, but in the high-velocity area, debonding takes over while the bonding process is still immature. Therefore the difference between Figs. 8 and 9 suggests that, for some reason, a difference arises in the process of bonding between the adhesive and the cylinder.

To compare the bonding process in the two adhesives, a measurement was made of the contact-time dependence of probe tack. Contact pressure (100g/cm^2) and pulling away velocity (1 cm/sec) remained constant. The rate of increase of effective contact area in the bonding process was calculated as conforming to the following equation:

$$dA(t)/dt = k[A(t) - A(0)]^n \tag{4}$$

where $A(t)$ is effective contact area at time (t), k is rate constant and n is rate order.

In the theories of W.M. Bright¹⁵⁾, K. Kanamaru¹⁶⁾ and J. Fukukawa¹⁷⁾ *et al.*, $n=1$, but the tolerance is reduced when n is used as general.

when $n=1$

$$A(t) = A(\infty) - \{A(\infty) - A(0)\} \exp(-kt) \tag{5}$$

where $n \neq 1$

$$A(t) = A(\infty) - \{A(\infty) - A(0)\}^{n+1} + (n-1)kt \cdot^{-1/(n-1)} \tag{6}$$

If activation energy is calculated by undertaking an Arrhenius plot of the rate constant k obtained by applying the curve of $n=4$ to the data obtained here, the result for PSA-N is $\Delta H^*_{\text{bond}} = 10\text{ kcal/mole}$ and for PSA-T 17 kcal/mole . Since activation energy values vary with n , a quantitative discussion is not possible, but in any case the ΔH^*_{bond} value of PSA-N is 1.5 to 2.0 times greater than that of PSA-T. In other words it is fairly certain that PSA-T has less wettability than PSA-N. We can now calculate rolling friction coefficient based on a simple model theory reflecting these findings.

When the cylinder rolls over the adhesive surface, contact is taken to begin from the lowest point of the cylinder ($\theta=0$) and proceed to $\theta=\theta_b$; if the apparent effective surface area of the side of the cylinder is taken as changing in accordance with the n th-degree speed formula, rolling friction coefficient can be expressed in the following equation⁹⁾:

$$f = (R^2 b / Mg) \int_0^{\theta_b} a(t) \cos \theta \sin \theta \, d\theta \tag{7}$$

where R , b and M are the radius, length and mass of the cylinder, $a(t) = A(t)/A(\infty)$, and $t = R\theta/v$.

If a dynamic equivalence model and failure conditions are established, the rolling friction coef-

ficient of an adhesive can be calculated using equations (7) and (5) or (6). Below is an example of the calculation curve when Hata's model is applied. The curves are master curves produced by shifting the rolling friction coefficient at high temperature (A), medium temperature (B) and low temperature (C) so as to superpose the low-velocity ranges where cohesive failure occurs.

Figure 11 is a curve plotted assuming equivalence of activation energy in the bonding and debonding processes (with each 1-digit decrease in dynamic relaxation time as temperature rises, the constant for rate of increase of effective contact area increases by one digit). Because the theoretical shape of the curve does not change with temperature, if the curves for A, B and C are shifted in line with the velocity axis, they can be superposed exactly.

Figure 12 meanwhile is a curve plotted assuming that activation energy in the bonding process is 1.5 times that of the debonding process (with each 1-digit decrease in dynamic relaxation time, the rate constant increases by 1.5 digits). Here, the temperature dependence of rolling friction coefficient in the high-velocity range varies with temperature, so that an overall master curve is not possible.

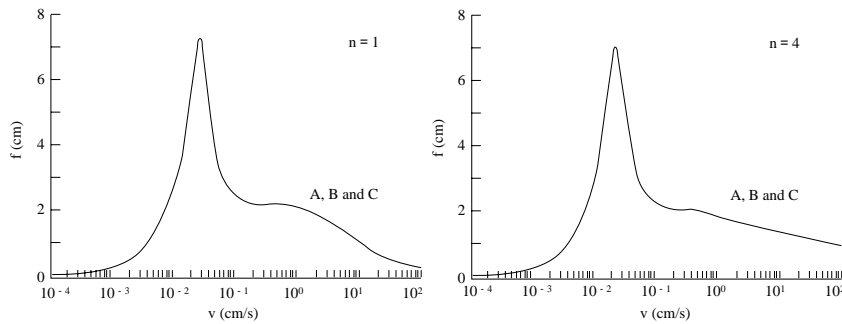


Fig. 11 Theoretical curve of rolling friction coefficient f assuming $H^*_{\text{bond}} = H^*_{\text{debond}}$
(Value of n is order of rate equation for bonding process)

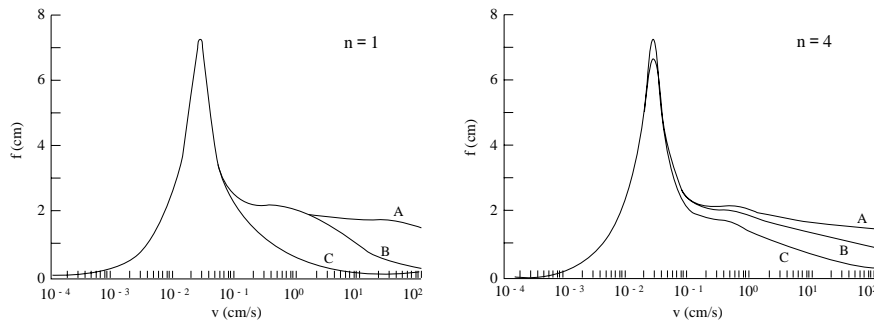


Fig. 12 Theoretical curve of rolling friction coefficient f assuming $H^*_{\text{bond}} = 1.5 \times H^*_{\text{debond}}$
(Value of n is order of rate equation for bonding process)

The difference between Figs. 8 and 9, that is, the finding that in the rolling friction coefficient of one of these two adhesives – in which copolymer composition, molecular weight and other chemical parameters are virtually equivalent - the velocity – temperature superposition law is applicable, while in the other it is only partially so, can be seen as suggesting that their debonding processes are the same but that the rates of their bonding processes differ slightly.

An ECSA analysis of the surfaces of the two adhesives revealed that while PSA-N was Si/C = 0.008, (Fig. 13), PSA-T was Si/C = 0.058 (Fig. 14). This seems likely to be the result of the dif-

ferent release agents used in the release liners of the two samples becoming transferred to some extent to the adhesive surface and thus influencing the bonding process between the cylinder and the adhesive surface. One possible view is that in the PSA-N system, the amount of transfer is small and its effect virtually negligible, while in the PSA-T system, the effect of the transfer cannot be disregarded. If this hypothesis is correct, measurement of rolling friction coefficient in the high-velocity range could be expected to be an effective method for clarifying the differences in the characteristics of the release agents.

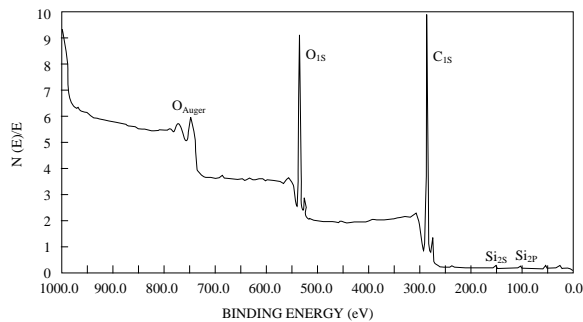


Fig. 13 ECSA spectrum of PSA-N

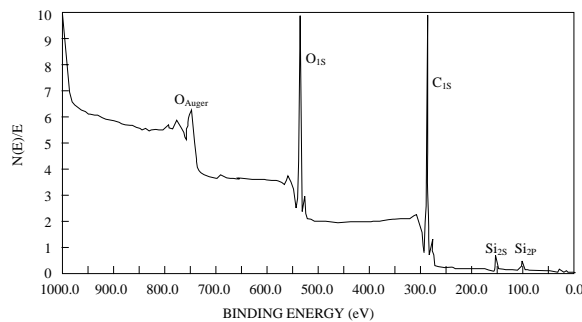


Fig. 14 ECSA spectrum of PSA-T

4. Conclusion

In the above the author has presented a discussion of adhesive tack. To accurately classify and evaluate the bonding and debonding processes between the adhesive and the adherend substrate and quantitatively account for the various phenomena of adhesion as they occur in actuality is an extremely difficult task. Accordingly the present paper has presented the two processes in an extremely simplified form.

To explain the mechanism producing tack in more detail and more rigorously in terms of physical science, it will be necessary to undertake basic research into its elementary processes.

For example in the probe tack test, when other conditions are held constant and only contact time is varied during measurement, resistance to pulling away (σ_{\max}) has an initial low value but increases with time and finally approaches a constant value. This suggests that a situation must be hypothesized in which, when the surface of an adherend of a certain apparent surface area contacts the adhesive surface, all the polymer segments at the interface do not instantaneously enter into an effective state of contact (that is, effective in exerting resistance); rather polymer segments which are in a non-effective state of contact seem gradually to transfer to an effective state.

There is existing research into the process by which polymer melt placed on a solid surface gradually spreads^{18), 19)}. However, there has been insufficient molecular theory research into the bonding process described in the preceding.

Regarding the debonding process, uniform deformation, cavity formation and expansion, fibrillation, interfacial failure, cohesive failure and other phenomena have been experimentally observed, but the related morphology and the physical criteria of the transfer of the failure process have not been clarified in all cases.

In recent times, direct measurement of surface force and mechanical testing at micro level have become possible^{20), 21)}. Meanwhile, it has also become possible to easily track morphological changes in materials in the leadup to failure. In the near future, it is hope that new insights into the various phenomena of bonding and adhesion will be gained leading to theoretical advances.

[References]

- 1) Adhesion Handbook, 3rd edition, The Adhesion Society of Japan edit., 1996, p.257.
- 2) F. Urushizaki, H. Yamaguchi, H. Mizumachi, *J. Adhesion Soc. Japan*, **20** (7), 295 (1984)
- 3) H. Mizumachi, T. Saito, *J. Adhesion*, **20**, 83 (1986)
- 4) H. Mizumachi, *Material Technology*, **2** (2), 72 (1984)
- 5) H. Mizumachi, Y. Hatano, *J. Adhesion*, **21**, 251 (1987)
- 6) H. Mizumachi, *J. Adhesion Soc. Japan*, **20** (11), 522 (1984)
- 7) T. Hata, T. Tsukatani, Y. Hatano, H. Mizumachi, *J. Adhesion Soc. Japan*, **30** (8), 352 (1994)
- 8) H. Mizumachi, *J. Appl. Polymer Sci.*, **30**, 2675 (1985)
- 9) H. Mizumachi, Y. Hatano, *J. Appl. Polym. Sci.*, **37**, 3097 (1989)
- 10) A. Zosel, Proc. Eurocoat Congress, p. 19 (1991)
- 11) H.-J. Kim, Ph. D. Dissertation, The University of Tokyo, 1995.
- 12) H. Lakrout, P. Sergot, C. Creton, *J. Adhesion*, **69**, 307 (1999)
- 13) A. Zosel, Proc. Int'l. PSA Technoforum, p. 51 (1997)
- 14) T. Tsukatani, Y. Hatano, H. Mizumachi, *J. Adhesion*, **31**, 59 (1989)
- 15) W. M. Bright, "Adhesion and Adhesives – fundamentals and practice" J. E. Rutler, Jr., and R. L. Savage ed., John Wiley and Sons, Inc., New York, N. Y. 1954 p. 130.
- 16) K. Kanamaru, *Kolloid – Z.*, **192**, 51 (1972)
- 17) J. Furukawa, Adhesion and Lamination, The Society of Polymer Science, Japan edit. Polymer Course 9, p. 196.
- 18) H. Shonhorn, H. L. Frisch, T. K. Kwei, *Appl. Phys.*, **37**, 4967 (1966)
- 19) T. Hata, Proc. Int'l. PSA Technoforum, p. 77 (1997)
- 20) J. Israelachvili, Book of Abstracts, WCARP – 1, p. 7 (1998)
- 21) A. V. Pocius, Introduction to Adhesion and Adhesive Technology, Hanser/Gardner Publication.